Scavenger receptor-B1 and luteal function in mice

Leonor Miranda Jiménez,[1,*] Mario Binelli,[1,*] Kalyne Bertolin,[*] R. Marc Pelletier,[†] and Bruce D. Murphy[2,*]

Centre de recherche en reproduction animale,* Faculté de médecine vétérinaire, and Departmente d'Anatomie et Pathobiology,† Université de Montréal, Québec, Canada

Abstract During luteinization, circulating high-density lipoproteins supply cholesterol to ovarian cells via the scavenger receptor-B1 (SCARB1). In the mouse, SCARB1 is expressed in cytoplasm and periphery of theca, granulosa, and cumulus cells of developing follicles and increases dramatically during formation of corpora lutea. Blockade of ovulation in mice with meloxicam, a prostaglandin synthase-2 inhibitor, resulted in follicles with oocytes entrapped in unexpanded cumulus complexes and with granulosa cells with luteinized morphology and expressing SCARB1 characteristic of luteinization. Mice bearing null mutation of the *Scarb1* gene (SCARB1$^{-/-}$) had ovaries with small corpora lutea, large follicles with hypertrophied theca cells, and follicular cysts with blood-filled cavities. Plasma progesterone concentrations were decreased 50% in mice with *Scarb1* gene disruption. When SCARB1$^{-/-}$ mice were treated with a combination of mevinolin [an inhibitor of 3-hydroxy-3-methylglutaryl CoA reductase (HMGR)] and chloroquine (an inhibitor of lysosomal processing of low-density lipoproteins), serum progesterone was further reduced. HMGR protein expression increased in SCARB1$^{-/-}$ mice, independent of treatment. It was concluded that theca, granulosa, and cumulus cells express SCARB1 during follicle development, but maximum expression depends on luteinization. Knockout of SCARB1$^{-/-}$ leads to ovarian pathology and suboptimal luteal steroidogenesis. Therefore, SCARB1 expression is essential for maintaining normal ovarian cholesterol homeostasis and luteal steroid synthesis.—Jiménez, L. M., M. Binelli, K. Bertolin, R. M. Pelletier, and B. D. Murphy. **Scavenger receptor B1 and luteal function in mice. *J. Lipid Res.* 2010.** 51: **2362–2371.**

Supplementary key words SCARB1 • luteinization • corpus luteum • 3-hydroxy-3-methylglutaryl CoA reductase

The cholesterol substrate required for most tissues to accomplish steroidogenesis exceeds the capacity for de novo synthesis of this sterol, and the principal means of augmentation of the supply is by importation of lipoprotein-bound cholesterol (1). Low-density lipoproteins enter cells by receptor-mediated endocytosis of the LDL complex and the LDL receptor (LDLR) (2). High-density lipoproteins interact with a membrane protein known as scavenger receptor-B1 (SCARB1) to effect the selective uptake of cholesterol esters from the HDL molecule into cells and the bidirectional transfer of free cholesterol (3). The relative contribution of LDL and HDL to the steroidogenic substrate pool varies among species and may vary among tissues within a species. One of the most active steroidogenic tissues is the corpus luteum (CL), formed from the components of the follicle following ovulation (4). In humans, circulating LDL is believed to be the major source of cholesterol for luteal steroid synthesis, but it has been shown that luteinized human granulosa cells can derive cholesterol esters from selective uptake via the HDL pathway (5). The HDL pathway appears to predominate in the CL of rodents (1), and SCARB1 is expressed in theca and luteal cells of the rat ovary (6). SCARB1 expression in primary cultures of rat granulosa cells is tightly coupled with the uptake of cholesterol esters, again suggesting that it is the major pathway for importation in this tissue (7). There is a low level of expression of SCARB1 in mouse granulosa cells (8), and recent studies of luteinization in the pig demonstrated similar low expression of SCARB1 in the granulosa cells of the follicle (9). The latter study revealed extensive upregulation of SCARB1 in the CL following ovulation, with a high level of expression persisting through the luteal phase. In the macaque, the ovulatory stimulus causes a rapid increase in expression of both SCARB1 and LDLR, but only LDL can augment steroidogenesis after 24 h in vitro (10).

This work was supported by an operating grant from the Canadian Institutes of Health Research (B.D.M.); by Consejo Nacional de Ciencia y Tecnología (CONACYT), México (L.M.J.); and by Fundcão de Amparo à Pesquisa do Estado de São Paulo and Coordenacão de Aperfeiçoamento de Pessoal de Nível Superior, Brazil (M.B.).

Manuscript received 22 March 2010 and in revised form 19 April 2010.

Published, JLR Papers in Press, April 19, 2010
DOI 10.1194/jlr.M006973

Abbreviations: CL, corpus luteum; DAPI, 4',6-diamidino-2-phenylindole; eCG, equine chorionic gonadotropin; hCG, human chorionic gonadotropin; HMGR, 3-hydroxy-3-methylglutaryl CoA reductase; LDLR, LDL receptor; PTGS2, prostaglandin synthase-2; SCARB1, scavenger receptor-B1.

[1] L. M. Jiménez and M. Binelli contributed equally to this article.

[2] To whom correspondence should be addressed.
e-mail: bruce.d.murphy@umontreal.ca

The inactivating mutation of SCARB1 in the mouse results in infertility, in the presence of a normal rate of ovulation (11) and a reportedly normal capacity to produce progestational steroids (12). The observation that nonviable oocytes are produced has led to the implication that the ovulatory process itself is disrupted in some way (11, 12). Although mechanisms remain unclear, it is intriguing that targeted overexpression of SCARB1 in the liver rescues fertility of SCARB1 null mice to nearly the levels found in wild-type mice (13). In addition, fertility was rescued by treatment with Probucol, a drug that lowers circulating cholesterol independent of SCARB1 (14). Further, if as noted above, the major supply of cholesterol for steroidogenesis in the CL is HDL imported via SCARB1 in mice, the means by which the ovary in the SCARB1 knockout mouse produces a functional CL remains unresolved.

Given the importance of SCARB1 to steroidogenesis and ovarian function, we explored the expression of SCARB1 in the ovary through the estrous cycle in adult mice and following blockade of ovulation in gonadotropin-stimulated immature mice. Further, to determine possible associations of form and function in the absence of a functional HDL importation system, we examined the morphology of ovarian structures and responses to pharmacological perturbations of the cholesterol metabolism in mice bearing inactivating mutation of SCARB1.

MATERIALS AND METHODS

Animals and tissue collection procedures

All animal experiments were approved by the Université de Montréal Animal Care Committee and conducted according to guidelines of the Canadian Council of Animal Care.

Our initial interest was to determine patterns of expression of SCARB1 in the ovary during final stages of follicular development and luteinization. Stages of the estrous cycle were determined in mature wild-type (WT) mice of mixed C56/B6 and Balb/c lineage by examination of exfoliative cytology of the vagina. Gene and protein expressions of SCARB1 were quantified in granulosa cells, and luteal tissues were obtained by laser microdissection as described in Duggavathi et al. (15). Briefly, ovaries (n = 3 mice in each of proestrus, estrus, and diestrus stages) were embedded in OCT compound (Tissue-Tek, Sakura Finetek USA, Inc., Torrance, CA), snap frozen in liquid nitrogen, and stored at −80°C. Frozen whole ovaries were cut using a Leica CM3050 Cryostat in 25 μM thick slices at −16°C and adhered to a polyethylene naphthalate-coated glass slide (Leica MicroDissect GmbH, Herborn, Germany). Tissues on slides were subsequently washed in PBS to remove OCT, stained in toluidine blue, dehydrated by washing in ethanol at increasing concentrations (70–100%), and incubated for 1 h at 37°C. The granulosa cell compartment was laser-microdissected from follicles present in ovaries collected from animals in proestrus and estrus stages of the estrous cycle, while the whole CL were microdissected from ovaries collected during diestrus. Laser-microdissection was performed using Leica AS LMD System at 20× magnification. From each animal, ovarian structures of one ovary were obtained for total RNA extraction by collection of microdissected fragments in RLT buffer (Qiagen RNeasy Micro Kit, Qiagen, Valencia, CA). Similar structures in the second ovary were collected for protein analysis following microdissection.

RNA and protein analysis

Total RNA was isolated from microdissected tissues as per manufacturer's instructions. For each sample, concentration of isolated total RNA was estimated from the absorbance measured at 260 nm using a NanoDrop apparatus (NanoDrop Technologies, Wilmington, DE), and the volume of extract containing 100 ng RNA was submitted to DNase treatment and reverse transcription. The resulting cDNA was used in subsequent qPCR reactions using a 7300 real-time PCR system (Applied Biosystems, Foster City, CA) conducted in triplicate, and each reaction contained 10 μl Power SYBR® Green PCR Master Mix (Applied Biosciences, Warrington, UK), 2 μl of a sense-antisense primer mix, 2 μl autoclaved ddH_2O, and 6 μl cDNA sample for a final volume of 20 μl. Common thermal cycling settings were used to amplify each transcript (2 min at 50°C, 10 min at 95°C, then 40 cycles of 15 s at 95°C and 60 s at 60°C). Melting-curve analyses were performed to verify product identity, adding a dissociation step to the PCR run (15 s at 95°C, 60 min at 60°C, 15 s at 95°C, and 15 s at 60°C). The sense and anti-sense sequences of primers for SCARB1 were 5′-TCTGGCGCTTTTTC-TATCGT-3′ and 5′-ACGGCCCATACCTCTAGCTT-3′ (16), each used in a final concentration of 300 nM. The ribosomal protein L19 (RPL19) was used for the normalization of SCARB1 abundance. The RPL19 primer sequences for sense and antisense primers were 5′- CTGAAGGTCAAAGGGAATGTG-3′and 5′-GGACAGAGTCTTGATGATCTC-3′ (17), each used in a final concentration of 300 nM. To test the efficiency of amplification of primers of each gene, a cDNA pool was made using equal volumes of cDNA solution from each sample. The cDNA pool was serially diluted in autoclaved ddH_2O from 1:7.5 to 1:240, and samples were analyzed using the qPCR procedure described above. Efficiency of amplification of each sample was estimated using the LinReg software (18), and the efficiency of amplification of the curve was obtained from the serially diluted cDNA calculated from the slope of the curve (http://efficiency.gene-quantification.info/). Calculated efficiencies ranged between 90 and 110% and were therefore considered adequate. Next, cDNA from each sample was diluted 1:10 in autoclaved ddH_2O and analyzed by qPCR for RPL19 and SCARB1. Relative abundance of SCARB1 transcripts was calculated by the ΔΔCt method corrected by the efficiency of amplification, as described by Pfaffl (19). The relative abundance of SCARB1 was analyzed by ANOVA using the procedure GLM from the software SAS (20). The independent variable was stage of the estrous cycle.

Ovarian structures of the remaining ovary were obtained for total protein extraction by collection of microdissected fragments in Laemmli buffer. Samples were boiled, centrifuged, and an equal volume (10 μl) of the supernatant of each sample submitted to SDS-PAGE. Proteins were subsequently blotted to a PVDF membrane. The membrane was blocked using 0.5% nonfat milk in tris-buffered saline containing 0.1% triton-X (TBST) for 1 h at room temperature, incubated with rabbit polyclonal anti-mouse SCARB1 (Novus Biologicals, Littleton, CO), diluted 1:5,000 in blocking solution overnight at 4°C, and finally incubated in HRP-conjugated goat anti-rabbit IgG (Jackson ImmunoResearch Laboratories, Inc.) diluted 1:100,000 in TBST for 1 h at room temperature. Proteins were visualized by chemiluminescence (Immobilon Western, Millipore Corporation, Billerica, MA). Subsequently, membranes were washed in TBST, blocked as above, and incubated with HRP-conjugated anti-mouse-β-actin (Santa Cruz Biotechnology, Santa Cruz, CA), diluted 1:50,000 in blocking solution for 20 min at room temperature. The optical density of bands detected at the expected molecular weight for SCARB1 and β-actin were quantified by the Image Processing and Analysis in Java (ImageJ) soft-

ware. The ratio of SCARB1 and β-actin densities was obtained for each sample and analyzed by ANOVA as described above.

Immunohistochemistry

To determine the distribution of SCARB1, ovaries were collected following euthanasia from three animals at each stage, dissected free from surrounding tissues under a stereoscope, fixed in paraformaldehyde, and embedded in paraffin using standard procedures. Ovarian tissue- and cell-specific localization of SCARB1 was verified by fluorescence immunohistochemistry. Briefly, paraffin sections of ovaries were rehydrated, boiled in 10 mM sodium citrate (pH 6.0) for 20 min, and cooled to room temperature (RT). Subsequently, sections were blocked in PBS containing 5% BSA for 30 min at RT, incubated with rabbit polyclonal anti-mouse SCARB1 (Novus Biologicals) or HMGR (Santa Cruz Biotechnology) diluted 1:50 in PBS containing 5% BSA overnight at 4°C. As a negative control, some sections were incubated with BSA in the place of SCARB antibody. Sections were washed, incubated with Cy3-conjugated goat anti-rabbit IgG (Jackson Immunoresearch Lab., Inc.), diluted 1:400 in PBS for 1 h at RT. Slides were then washed, and sections were counterstained with 4',6-diamidino-2-phenylindole (DAPI, Sigma, St. Louis, MO), diluted 1:1000 in PBS, for 5 min. Slides were mounted in Permafluor (Lab Vision Corp., Fremont, CA). Ovarian distribution of SCARB1 was observed by confocal microscopy using the Olympus Fluoview 1000 system and Fluoview version 1.7 software. Laser sources of 543 nM and 405 nM were employed for detection of CY3 and DAPI signals, respectively. For a given fluorochrome (i.e., CY3 or DAPI), photomultiplier voltage, laser power, pinhole aperture, time of acquisition, and image resolution were maintained constant for all confocal images. The Kalman filter mode was used for all image acquisition. For high magnification images (600×) of follicles, "stacks" of five subsequent images, 1.42 mm thick each, were obtained. Then, for each particular cell type (i.e., theca, mural granulosa, or cumulus), the image within the stack showing the strongest signal was selected for analysis.

Experimental procedures

Experiment 1. To determine whether the elevated expression of SCARB1 that accompanies luteinization depends on ovulation, immature WT female mice received IP injections of equine chorionic gonadotropin (eCG; 5 IU) to induce follicular development, followed by human chorionic gonadotropin (hCG; 5 IU) 48 h later to induce ovulation. At 4 h prior to the hCG injection, animals received 0 or 6 mg/g body weight (BW) meloxicam [MEL; prostaglandin synthase-2, (PTGS2) activity inhibitor; Sigma, St. Louis, MO] to block ovulation (21). Ovaries and oviducts were collected 18, 24, or 36 h after the hCG injection (n = 3 animals/time point) and separated by dissection. Oviducts and the right ovary of each mouse were embedded in paraffin. Morphology of ovarian structures and presence of ovulated oocytes in oviducts were observed by light microscopy in hematoxlyn/eosin (HE)- or periodic acid-Schiff (PAS)-stained tissue sections. Ovarian tissue- and cell-specific localization of SCARB1 was verified by fluorescence immunohistochemistry and confocal microscopy. The left ovary of each mouse was snap frozen in liquid nitrogen and stored at −80°C until RNA extraction and real-time PCR (qPCR) was carried out, except that for each sample, the volume of extract containing 1 μg RNA was submitted to DNase treatment and reverse transcription. The relative abundance of SCARB1 was analyzed by ANOVA using the GLM procedure from SAS software (20). Independent variables were treatment (placebo or MEL), time after hCG injection (18, 24, or 36 h), and the treatment by time interaction.

Experiment 2. Given the central role of SCARB1 in ovarian steroidogenesis, a SCARB1$^{-/-}$ mouse model provided by Dr. M. Krieger (11) was used to examine the effects of SCARB1 absence on ovarian morphology. Development and ovulation of follicles in adult, wild-type (WT), and SCARB1$^{-/-}$ mice were stimulated with eCG and hCG injections 48 h apart. Cholesterol supply was further perturbed by pharmaceutical intervention with de novo synthesis and delivery of cholesterol from LDL. At 4 h prior to hCG injection, animals were divided to receive vehicle or a combination of 20 μg/g BW mevinolin (Mev), an inhibitor of 3-hydroxy-3-methyl-glutaryl-CoA reductase (HMGR; Sigma, Fair Lawn, NJ) and 100 μg/g BW of chloroquine (Chloro; Science Lab, Inc., Kingwood, TX), a weak base that interferes with cholesterol efflux from lysosomes, thereby inhibiting intracellular delivery of cholesterol from LDL (22, 23). The experiment took the form of a 2 × 2 factorial (n = 3 per group). Ovaries and blood were collected 18 h after the hCG injection, the former fixed in Bouin's solution for 24 h and embedded in paraffin as described earlier. Morphology of ovarian structures was observed by light microscopy both in HE- and PAS-stained tissue sections. To verify whether inhibiting cholesterol sources affected ovarian tissue- and cell-specific localization of SCARB1 in WT mice, SCARB1 was identified by immunohistochemistry, as described for experiment 1. Because manipulating cholesterol sources was expected to alter expression of cholesterol synthesizing enzymes, ovarian abundance and distribution of HMGR was analyzed in all animals by immunohistochemistry. The procedure was similar to that described above for detection of SCARB1, except that a goat anti-human polyclonal antibody (Santa Cruz Biotechnology), diluted 1:50 in PBS containing 5% BSA, and a CY3-conjugated donkey anti-goat IgG antibody (Jackson Immunoresearch Lab, Inc.), diluted 1:400 in PBS, were employed.

Hormone assay

Progesterone concentrations in serum were evaluated in a single radioimmunoassay according to a protocol described previously (15). The intra-assay coefficient of variation was cal-

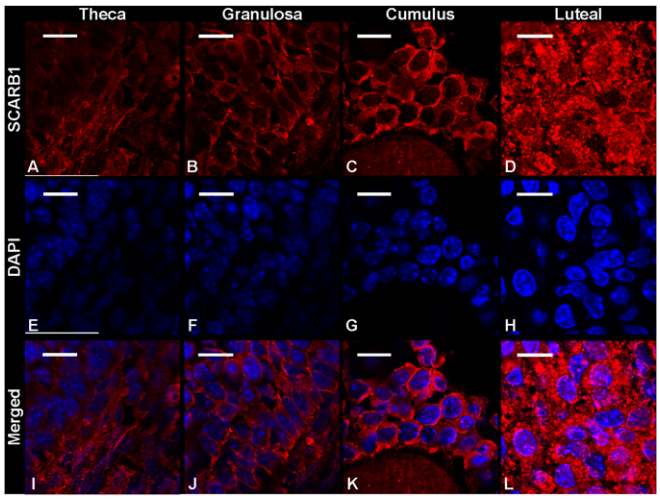

Fig. 1. Protein expression of SCARB1 in the ovarian theca (A), granulosa (B), cumulus oophorus (C), and luteal cells (D) of mature mice undergoing normal estrous cycles. A–D: Confocal microscopy images of fluorescent immunohistochemistry staining of SCARB1. E–H: Confocal microscopy images of DAPI staining of nuclei. I–L: Merged image of SCARB1 and DAPI. Bars: 10 μm. Images are representative of the ovaries of three or more animals. DAPI, 4',6-diamidino-2-phenylindole; SCARB1, scavenger receptor-BI.

culated between duplicates ranging from 1% to 9%. Concentrations of progesterone were analyzed by ANOVA using the procedure GLM from SAS software (20). Independent variables were genotype (WT or SCARB1$^{-/-}$), treatment (control or Chloro/Mev combination), and the genotype by treatment interaction.

RESULTS

Distribution of SCARB1 through the mouse estrous cycle

Immunohistochemical analysis revealed punctate expression SCARB1 in theca, mural granulosa, cumulus, and

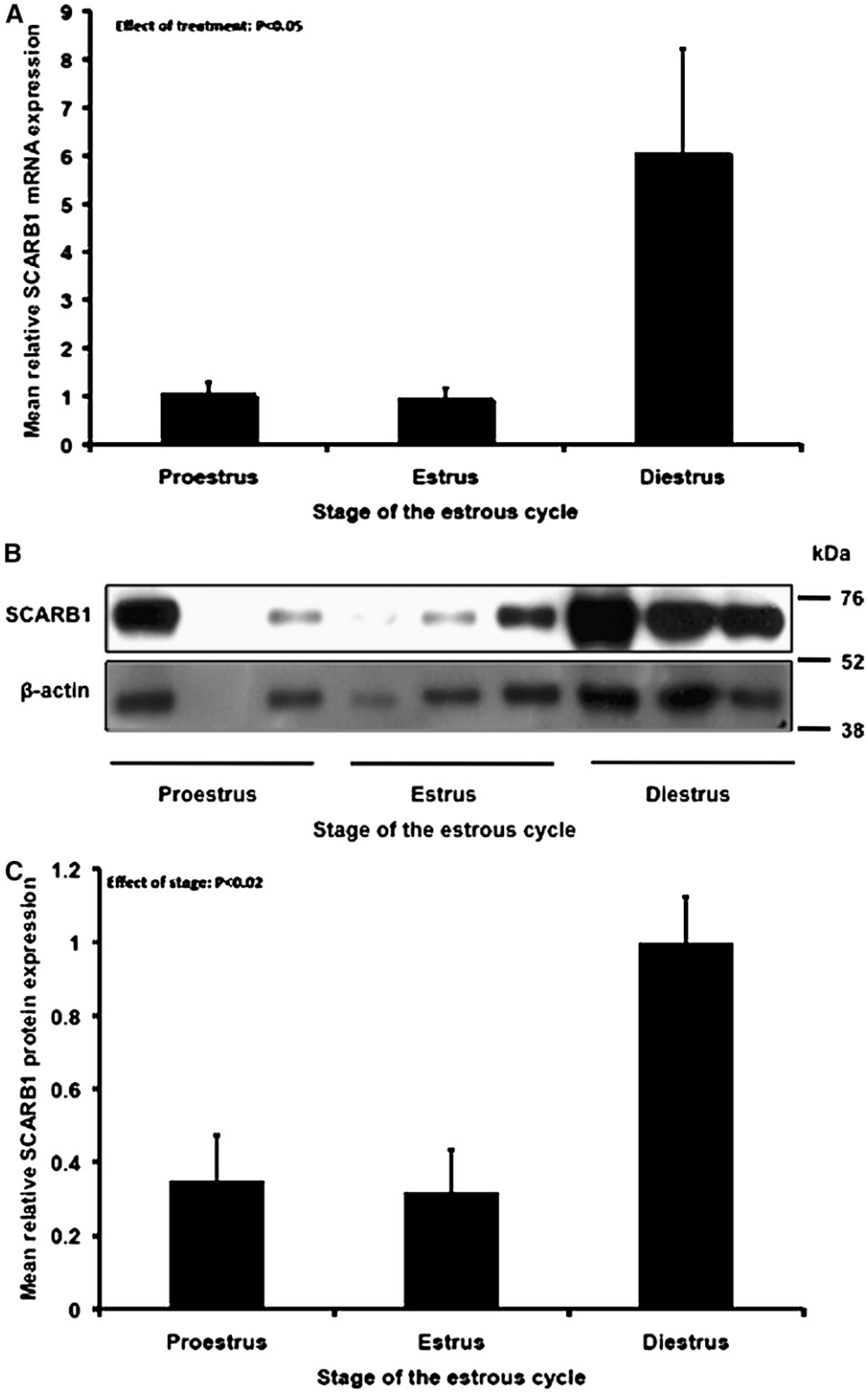

Fig. 2. Relative abundance of SCARB1 mRNA (A) (means ± SEM) and protein (B, C) in ovarian cells collected by laser microdissection from ovaries collected at different stages of the estrous cycle from WT mice, as determined by qPCR and immunoblotting. SCARB1, scavenger receptor-BI; WT, wild type.

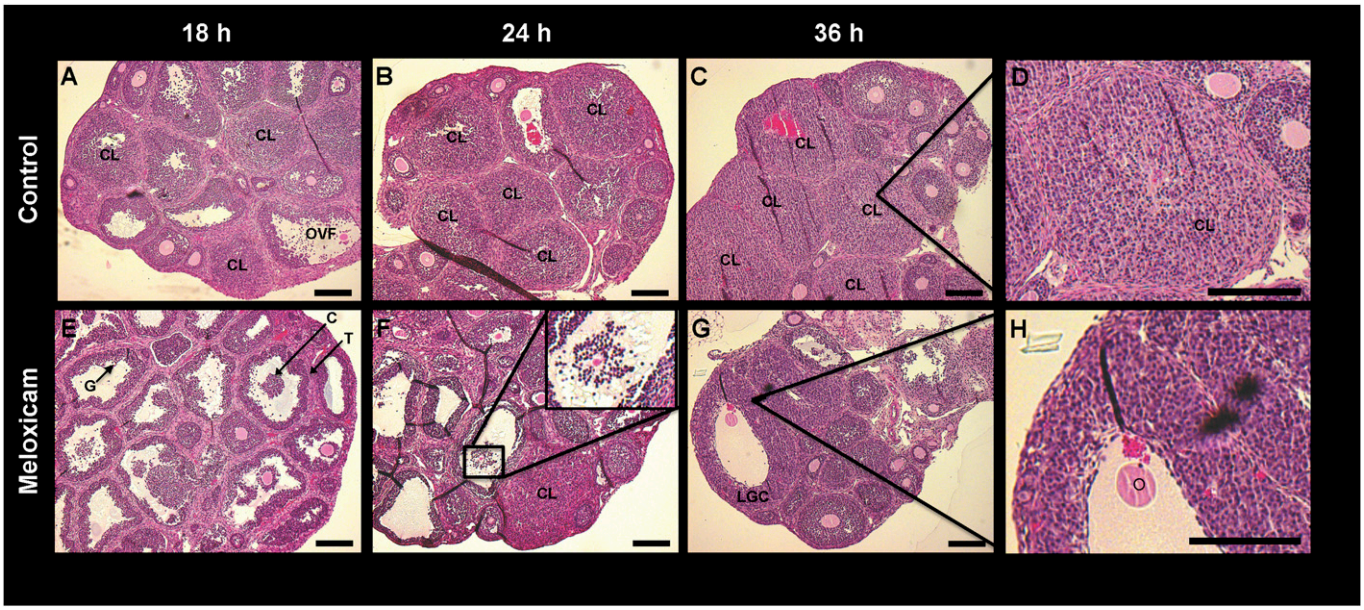

Fig. 3. Bright field microscopy images of hematoxylin-eosin stained sections of ovaries from immature mice stimulated with equine chorionic gonadotropin (eCG) and human chorionic gonadotropin (hCG) and collected 18 h (A, E), 24 h (B, F) or 36 h after hCG (C, G). Mice received 0 (A–D) or 6 mg/g body weight meloxicam, a prostaglandin synthase-2 activity inhibitor (E–H). D: An enlargement of a CL at 36 h after hCG. H: Intact follicle with luteinized granulosa cells and entrapped oocyte at 36 h after hCG in a meloxicam-treated mouse. F insert: An oocyte with expanded cumulus oophorus. Bars: 150 μm. C, cumulus oophorus; CL, corpus luteum; G, granulosa cells, O, oocyte T, theca.

luteal cells (**Fig. 1**). In all cell types, expression was observed throughout the cytoplasm and plasma membrane but appeared absent from the nucleus. Staining was more intense in the cytoplasm of luteal cells, and given the larger volume of cytoplasm with respect to follicular cells, it was clear that SCARB1 protein expression per cell is greater in the cells of the CL. Overall, SCARB1 expression appeared to be similar as follicles developed from proestrus to estrus, and expression increased drastically following luteinization (Fig. 1). This trend was confirmed in laser microdissected ovarian tissue collected at specific stages of the estrous cycle. Indeed, SCARB1 mRNA relative abundance increased 6-fold ($P < 0.05$) as animals progressed from proestrus-estrus to diestrus (**Fig. 2A**). Furthermore, the SCARB1 protein abundance, as estimated by Western blotting, followed a similar pattern of increase (Fig. 2B, C).

Ovulatory patterns

To further establish the expression patterns of SCARB1 and determine the role of ovulation in the increase of the SCARB1 gene expression and immunoreactivity, we treated mice with MEL, the inhibitor of PTGS2 activity, or with vehicle. Histological analysis of the ovaries (**Fig. 3**) and oviducts (data not shown) revealed that ovulation had occurred in all but a few large follicles in the vehicle-treated animals by 18 h after hCG treatment. The expected CL formation was evident in control animals at 24 and 36 h (Fig. 3A–D). In contrast, the ovaries of mice treated with MEL displayed oocytes surrounded by compact layers of cumulus cells in follicles and no corpora lutea at 18 h after hCG treatment; antral follicles with entrapped oocytes and a few corpora lutea at 24 h; and oocytes entrapped in follicles with reduced or absent antra at 36 h (Fig. 3E–H). In the MEL-treated mice, the granulosa layer at 36 h after hCG appeared 2-fold thicker or more than in preovulatory follicles (Fig. 3H).

Ovarian abundance of SCARB1 mRNA increased over time after hCG injection and was at a maximum at 36 h (effect of time; $P < 0.01$) (**Fig. 4**). Increases occurred regardless of MEL treatment (no treatment by time interaction), indicating that blocking ovulation did not interfere with whole ovary SCARB1 expression. SCARB1 protein immunolocalization indicated that MEL treatment induced a

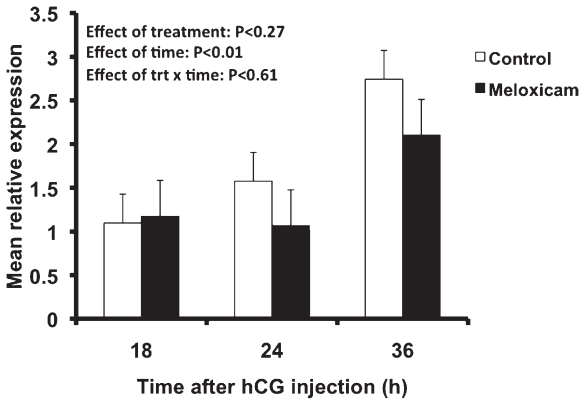

Fig. 4. Relative abundance of SCARB1 mRNA (means ± SEM) as determined by qPCR in whole ovaries collected 18, 24, or 36 h after hCG of immature mice stimulated with eCG and hCG. Mice received 0 (Control; open bars) or 6 μg/g BW meloxicam, a cyclooxygenase-2 activity inhibitor (Meloxicam; solid bars). eCG, equine chorionic gonadotropin; hCG, human chorionic gonadotropin; SCARB1, scavenger receptor-B1.

redistribution of the SCARB1 signal among ovarian structures. In the ovaries of vehicle-treated mice, the signal for SCARB1 was found in the cytoplasm of granulosa cells at 18 h after the ovulatory stimulus and appeared not to vary at 24 h or 36 h (data not shown). The granulosa cells maintained expression levels not different from proestrus (Figs. 1 and 2). In contrast, immunoreactivity in luteal cells (present in corpora lutea, defined by the absence of an oocyte, vascularization of the former granulosa cell layer, and increased nuclear/cytoplasmic ratio relative to granulosa cells) appeared to increase across time **Fig. 5A**–C). In ovaries from animals in which ovulation was blocked with MEL, the onset of increased expression of SCARB1 in nonovulated follicles, as visualized by confocal microscopy, occurred at 18 h (Fig. 5D–F). By 36 h, the cells in the thickened mural granulosa layer displayed an increase in cell volume and the presence of foamy cytoplasm characteristic of luteal cells. The SCARB1 expression was consistent with luteinization, in spite of the absence of ovulation and entrapment of the oocyte. In the few follicles that ovulated in MEL-treated mice, the signal was similar to that seen in granulosa cells of the vehicle-treated controls at 24 h (Fig. 5G). At 36 h, the luteal phenotype was emerging in these few follicles, but it appeared to be delayed relative to the control CL, in that there was an apparently lower expression of SCARB1 (Fig. 5H).

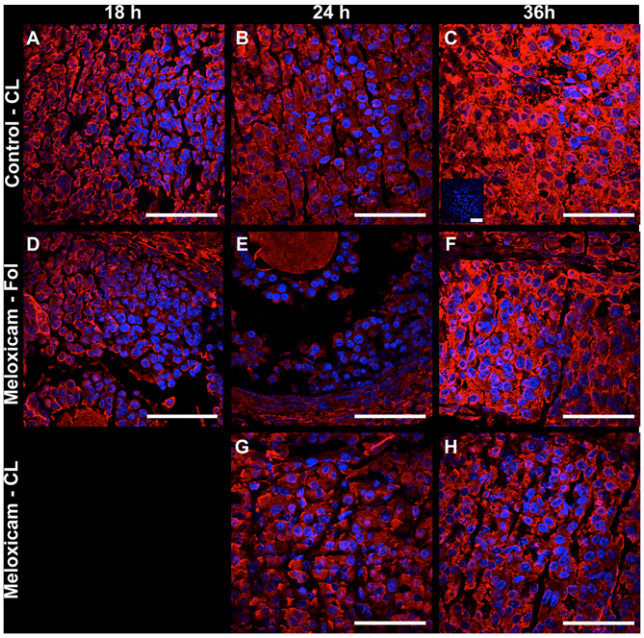

Fig. 5. Protein expression of SCARB1 in representative corpora lutea (A–C, G, H) and in follicles (D–F) of immature mice stimulated with eCG and hCG and collected 18 h (A, D), 24 h(B, E, G) or 36 h after hCG (C, F, H). Mice received 0 (A–C) or 6 μg/g BW meloxicam, a prostaglandin synthase-2 activity inhibitor (D–H). Merged confocal microscopy images of fluorescent immunohistochemistry staining of SCARB1 and DAPI staining of nuclei. Panel C insert: An example of negative control (first antibody replaced by BSA). Bars: 50 μm. eCG, equine chorionic gonadotropin; hCG, human chorionic gonadotropin; SCARB1, scavenger receptor-B1.

Effects of reduction of cholesterol supply

Previous reports suggest that there is no luteal defect in mice bearing null mutation of the SCARB1 gene. In contrast, we found that circulating progesterone levels in serum samples of superstimulated, ovulated mice were lower in SCARB1 knockout mice by approximately 50% compared with the WT ($P < 0.01$) during the luteal phase (**Fig. 6**). It was therefore of interest to determine whether there are morphological correlates in ovaries of SCARB1$^{-/-}$ mice related to reduced progesterone output.

The ovaries in the SCARB1$^{-/-}$ mice examined consistently displayed abnormal structures not found in WT ovaries. The first was a blood-filled follicular cyst (**Fig. 7A**). This structure was present in various degrees of enlargement throughout the SCARB1$^{-/-}$ ovaries. At 18 h after hCG injection and approximately 6 h after expected ovulation, ovaries from SCARB1$^{-/-}$ mice contained some structurally normal corpora lutea and smaller luteinized structures. (Fig. 7B). A common finding was the presence of follicle-like structures that appeared to have two layers, with the outer comprising hypertrophied, luteal-like cells and the interior resembling the granulosa cell compartment of a normal follicle (Fig. 7C). To further define this structure, ovarian sections were stained with PAS to reveal polysaccharides. This analysis revealed an intact basement membrane (Fig. 7D) between the outer and inner compartments, leading to the conclusion that this structure is an intact follicle with a hypertrophied theca compartment.

We then attempted to further reduce the cholesterol pool in SCARB1$^{-/-}$ and WT mice by blocking de novo synthesis with Mev and interdicting LDL processing with Chloro. Overall, this treatment reduced circulating progesterone 42% ($P < 0.02$). Reduction was 43% in WT mice and 30% in SCARB1$^{-/-}$ (Fig. 6). No effect of the combined treatment on luteal morphology was evident in ovaries harvested from either the WT or SCARB1$^{-/-}$ mice (**Fig. 8**). To further explore the means by which SCARB1$^{-/-}$ mice compensate for the deficiency in HDL uptake, we examined the abundance of signal for HMGR, a rate-limiting enzyme in the cholesterol pathway, in the luteal structure in WT and SCARB1$^{-/-}$ mice by fluorescent immunohistochemistry and confocal microscopy. The intensity of fluorescence indicates that HDL deficiency in SCARB1$^{-/-}$ mice results in increased expression of this enzyme (**Fig. 9**). Blockade of HMGR activity and concurrent interference with LDL metabolism had no apparent effect on the abundance of the HMGR cellular protein in the WT mice. In contrast, the expression of the cholesterol synthetic enzyme appeared more intense in the Mev/Chloro-treated SCARB1$^{-/-}$ mice. This finding further supports the view that increased HMGR expression is a major mechanism by which SCARB1$^{-/-}$ mice obtain the cholesterol required for luteal steroid synthesis.

DISCUSSION

The pattern of expression of SCARB1 in the mouse follicle differs from the pig (9), the other species where it has been examined in detail, in that there is substantial signal present in the granulosa cells throughout the estrous

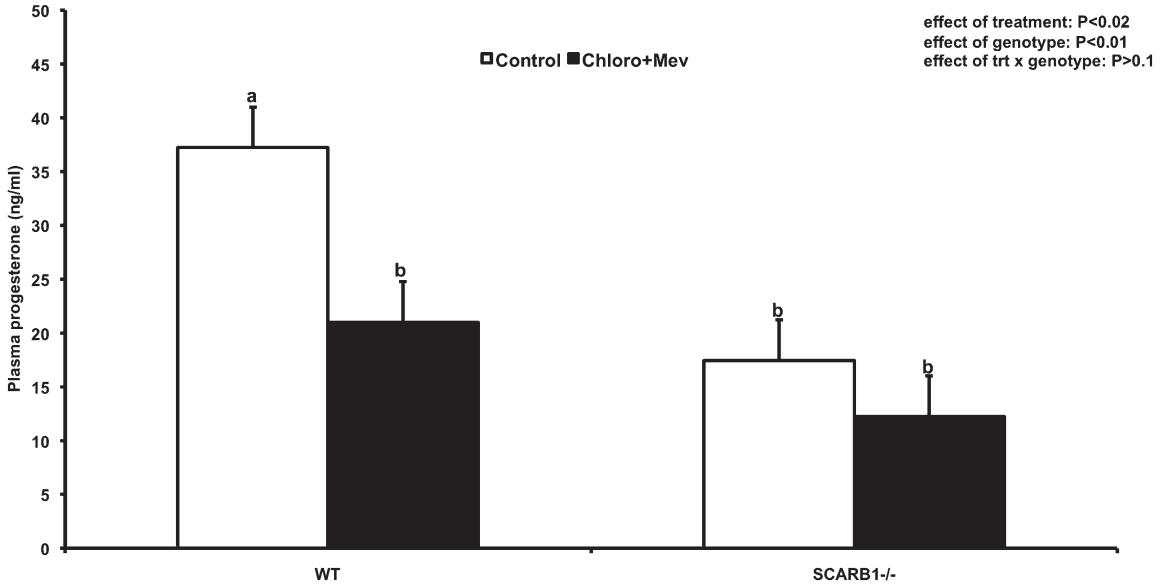

Fig. 6. Plasma progesterone concentrations (LS means ± SEM) from WT or SCARB1$^{-/-}$ mature mice stimulated with eCG and hCG and collected 18 h after hCG. Mice received placebo injections (Control) or a combination of 20 mg/g BW mevinolin (Mev; an HMGR inhibitor) and 100 mg/g BW chloroquine (Chloro; an inhibitor of lysosomal processing of LDL). hCG, human chorionic gonadotropin; HMGR, 3-hydroxy-3-methylglutaryl CoA reductase; eCG, equine chorionic gonadotropin; hCG, human chorionic gonadotropin; SCARB1, scavenger receptor-B1; WT, wild type.

cycle. The protein was found in the cytoplasm and at the periphery of both granulosa and luteal cells in the mouse. Strong cytoplasmic expression in granulosa cells is in contrast to the pig findings, where there was a low level of punctate expression in the cytoplasm and a primarily peripheral localization of the protein (9). This difference may reflect, in part, differences in the method of detection, because in another study, conventional microscopy demonstrated SCARB1 to be localized on the apical membrane of the enterocyte, while confocal microscopy revealed both cytoplasmic and membrane distribution (24).

We further observed strong SCARB1 expression in the cumulus oophorus of the follicle, consistent with the view that the cumulus serves as an important source of cholesterol for the maturing oocyte (25). The distribution of the protein suggests SCARB1 may play an important role in uptake of HDL from the follicular fluid and consequent efflux to the oocyte. The SCARB1$^{-/-}$ mouse, while capable of ovulation, is infertile due to so far unexplained oocyte defects that prevent fertilization (12). This infertility is reversed by transplant of the ovaries to the WT females (12) or by induction of hepatic SCARB1 expression in the

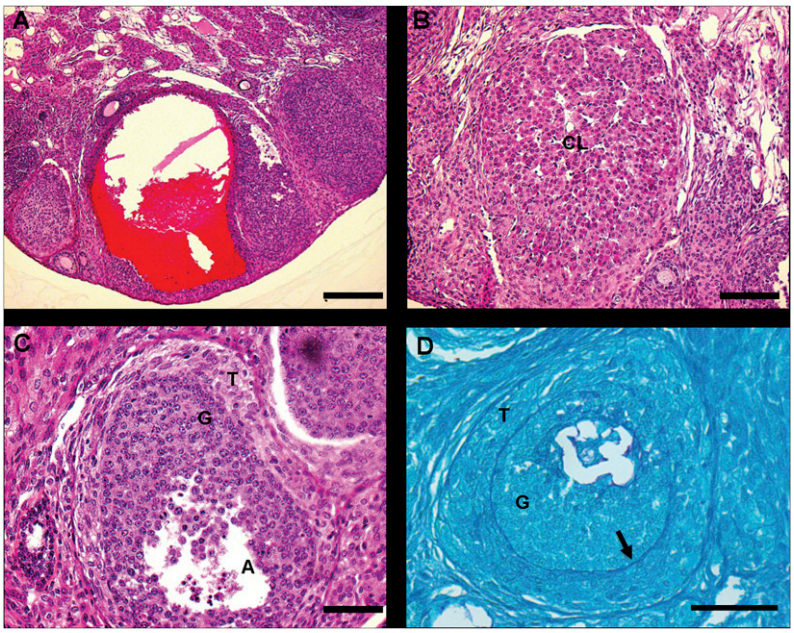

Fig. 7. Bright field microscopy images of atypical structures in hematoxylin-eosin-stained (A–C) or periodic acid-Schiff (PAS)-stained (D) sections of ovaries from SCARB1$^{-/-}$ mature mice stimulated with eCG and hCG and collected 18 h after hCG. A: Follicular cyst-like structure; bar: 200 μm. B: Small luteinized structure; bar: 100 mm. C: Partially luteinized follicle; bar: 50 μm. D: Partially luteinized follicle showing intact basal lamina (arrow); bar: 50 μm. CL, corpus luteum; eCG, equine chorionic gonadotropin; G, granulosa cells; hCG, human chorionic gonadotropin; SCARB1, scavenger receptor-B1; T, theca.

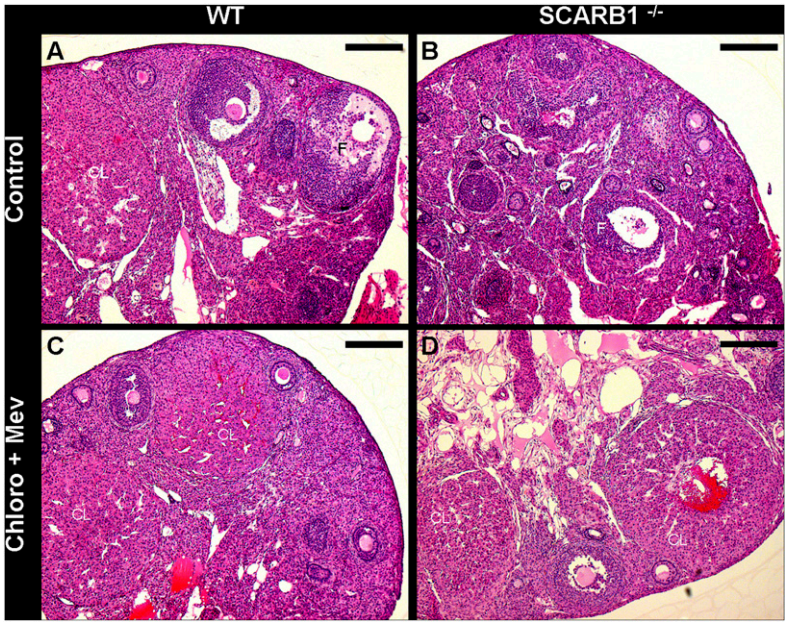

Fig. 8. Bright field microscopy images of hematoxylin-eosin-stained sections of ovaries from WT (A, C) or SCARB1$^{-/-}$ mature mice stimulated with eCG and hCG and collected 18 h after hCG. Mice received placebo injections (A, B) or a combination of 20 μg/g BW mevinolin (Mev; an HMGR inhibitor) and 100 μg/g BW chloroquine (Chloro; an inhibitor of lysosomal processing of LDL) (C, D). Bars: 200 μm. CL, corpus luteum; eCG, equine chorionic gonadotropin; F, follicle; hCG, human chorionic gonadotropin; HMGR, 3-hydroxy-3-methylglutaryl CoA reductase; SCARB1, scavenger receptor-B1; WT, wild type.

liver alone (13). These findings are consistent with the conclusion that dyslipidemia and inappropriate transfer of HDL cholesterol between the cumulus cells and the oocyte impair normal oocyte development, thereby rendering the ovulated ovum not fertilizable.

To explore the role of ovulation and luteinization in SCARB1 expression, we employed a pharmacological blockade of PTGS2, an enzyme well known to be necessary for the ovulatory process (26). The qPCR results indicate that the process of SCARB1 expression in the ovary occurs in the absence of ovulation and on a similar time scale. Moreover, dynamics of SCARB1 expression in relation to hCG injection were similar between treatments. This is intriguing because CLs are the ovarian structures with greatest SCARB1 expression, and they were present in a lower number in MEL-treated mice in all time points studied. Fluorescent immunohistochemistry analysis permitted us to observe a redistribution of the SCARB1 signal caused by MEL treatment. Specifically, the SCARB1 signal became more intense in nonovulated follicles in the MEL group, while the morphological observations indicated that the granulosa cells therein luteinized. The rare follicles that ovulated following MEL treatment appeared delayed in expression of SCARB1, suggesting that, in a few cases, the treatment retarded ovulation.

Western analysis confirmed the absence of the SCARB1 protein in the SCARB1$^{-/-}$ mouse. In contrast to previous reports that indicate no differences in ovarian morphology between null and WT mice and no reduction in circulating progesterone (11), our findings suggest significant pathology in the SCARB1$^{-/-}$ mouse ovary. Some corpora lutea were smaller in diameter than those in WT animals. There were large cystic, hemorrhagic follicles that resembled structures in mice with null mutation of the estrogen receptor-α gene *(Esr1)* (27), suggesting that estrogen deficiency may play a role in the phenotype. The defect may be earlier in the steroidogenic pathway. It is known that progesterone is required for ovulation (28), and it is possible that the absence of SCARB1compromises granulosa cell steroidogenesis that ensues after the ovulatory stimulus.

A further structure, represented by an intact granulosa compartment surrounded by a hypertrophied theca, was common in the ovaries of the SCARB1$^{-/-}$ mouse. The basis for this anomaly is unclear, but follicles with similar morphology can be found in a mouse model engineered to overexpress the luteinizing hormone-β subunit and thus are hyperandrogenic (29). Given the important role of SCARB1 in thecal androgen production (30), the alternative—that these cells produce only low levels of androgens—is possible.

We examined the effects of reducing the availability of cholesterol by concurrent interdiction of de novo synthesis and interference with lyosomal processing of LDL. This combined treatment had no apparent effect on the morphology of the ovaries, and reduced, but did not eliminate, circulating progesterone in both WT and SCARB1$^{-/-}$ mice. The increased expression of HMGR in the SCARB1$^{-/-}$ ovary was interpreted to be an intracellular feedback response to the reduction in intracellular cholesterol in the transgenic ovaries (31). The mouse bearing spontaneous mutation in the Niemann-Pick C1 gene is unable to process LDL cholesterol but displays circulating progesterone concentrations that do not differ from WT mice (32). The dysfunction of the LDL pathway is compensated, presumably by de novo synthesis of cholesterol and its importation via SCARB1. As all three sources were believed to have been compromised in the present study, it must be concluded that cholesterol stored in the CL in the form of cholestryl esters was the source of the substrate for progesterone synthesis.

The feedback system for cholesterol homeostasis is regulated by the abundance of the transcriptionally active form of sterol-regulatory element binding protein (SREBP) (31). An important transcriptional target of SREBP is the

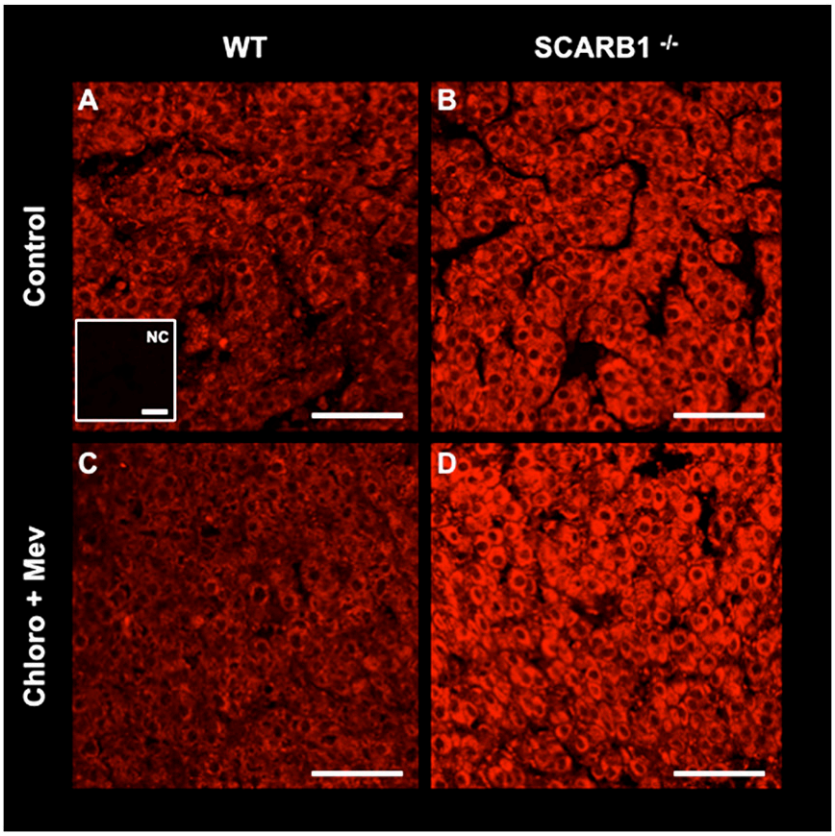

Fig. 9. Immunohistochemistry of HMGR, the rate-limiting enzyme in cholesterol synthesis, in corpora lutea from WT (A, C) or SCARB1$^{-/-}$ mature mice (B, D) stimulated with eCG and hCG and collected 18 h after hCG. Mice received placebo injections (A, B) or a combination of 20 μg/g BW mevinolin (Mev; an HMGR inhibitor) and 100 μg/g BW chloroquine (Chloro; an inhibitor of lysosomal processing of LDL) (C, D). A insert: Negative control (NC) for the SCARB1 immunofluorescence staining reaction where the first antibody was omitted. Bars: 50 μm. eCG, equine chorionic gonadotropin; hCG, human chorionic gonadotropin; HMGR, 3-hydroxy-3-methylglutaryl CoA reductase; SCARB1, scavenger receptor-B1; WT, wild type.

HMGR gene, and evidence from the present investigation indicates that its expression is elevated in the SCARB1$^{-/-}$ mouse CL. This concurs with the idea that inactivation of an import pathway, as occurs in the NPC-1 mutant mouse, is compensated by increased de novo cholesterol synthesis. Immunohistochemical analysis suggested an even greater expression of HMGR when there was interdiction of both the HDL and LDL import pathways. It would appear that increased HMGR expression is a major alternative to supply cholesterol for luteal steroidogenesis.

SUMMARY

We have shown an increasing, predominantly cytoplasmic SCARB1 protein expression in theca and granulosa cells in the mouse ovary during the final stages of follicle growth, with expression becoming maximal as follicular cells luteinize in response to the ovulatory stimulus. Lack of a functional SCARB1 protein resulted in morphological aberrations of follicular structures in the ovary and reduction in progesterone synthesis. Intraovarian cholesterol synthetic mechanisms can compensate, at least in the short term, for a nonfunctional cholesterol import system.

The authors thank Vickie Roussel, Catherine Dolbec, Hamid Reza Kohan-Ghadr; and Mira Dobias for technical assistance; Drs. Patrick Vincent and Lawrence Smith for aid with confocal microscopy; and Drs. Monte Krieger and Louise Brissette for contribution of SCARB1 mice.

REFERENCES

1. Murphy, B. D., and S. L. Silavin. 1989. Luteotrophic agents and steroid substrate utilization. *Oxf. Rev. Reprod. Biol.* **11:** 179–223.
2. Goldstein, J. L., and M. S. Brown. 1985. The LDL receptor and the regulation of cellular cholesterol metabolism. *J. Cell Sci. Suppl.* **3:** 131–137.
3. Connelly, M. A., and D. L. Williams. 2004. Scavenger receptor BI: a scavenger receptor with a mission to transport high density lipoprotein lipids. *Curr. Opin. Lipidol.* **15:** 287–295.
4. Murphy, B. D. 2000. Models of luteinization. *Biol. Reprod.* **63:** 2–11.
5. Azhar, S., L. Tsai, S. Medicherla, Y. Chandrasekher, L. Giudice, and E. Reaven. 1998. Human granulosa cells use high density lipoprotein cholesterol for steroidogenesis. *J. Clin. Endocrinol. Metab.* **83:** 983–991.
6. Li, X., H. Peegel, and K. M. Menon. 1998. In situ hybridization of high density lipoprotein (scavenger, type 1) receptor messenger ribonucleic acid (mRNA) during folliculogenesis and luteinization: evidence for mRNA expression and induction by human chorionic gonadotropin specifically in cell types that use cholesterol for steroidogenesis. *Endocrinology.* **139:** 3043–3049.

7. Azhar, S., A. Nomoto, S. Leers-Sucheta, and E. Reaven. 1998. Simultaneous induction of an HDL receptor protein (SR-BI) and the selective uptake of HDL-cholesteryl esters in a physiologically relevant steroidogenic cell model. *J. Lipid Res.* **39:** 1616–1628.
8. Reaven, E., Y. Lua, A. Nomoto, R. Temel, D. L. Williams, D. R. van der Westhuyzen, and S. Azhar. 1999. The selective pathway and a high-density lipoprotein receptor (SR-BI) in ovarian granulosa cells of the mouse. *Biochim. Biophys. Acta.* **1436:** 565–576.
9. Miranda-Jimenez, L., and B. D. Murphy. 2007. Lipoprotein receptor expression during luteinization of the ovarian follicle. *Am. J. Physiol. Endocrinol. Metab.* **293:** E1053–E1061.
10. Cherian-Shaw, M., M. Puttabyatappa, E. Greason, A. Rodriguez, C. A. VandeVoort, and C. L. Chaffin. 2009. Expression of scavenger receptor-BI and low-density lipoprotein receptor and differential use of lipoproteins to support early steroidogenesis in luteinizing macaque granulosa cells. *Endocrinology.* **150:** 957–965.
11. Trigatti, B., H. Rayburn, M. Vinals, A. Braun, H. Miettinen, M. Penman, M. Hertz, M. Schrenzel, L. Amigo, A. Rigotti, et al. 1999. Influence of the high density lipoprotein receptor SR-BI on reproductive and cardiovascular pathophysiology. *Proc. Natl. Acad. Sci. USA.* **96:** 9322–9327.
12. Miettinen, H. E., H. Rayburn, and M. Krieger. 2001. Abnormal lipoprotein metabolism and reversible female infertility in HDL receptor (SR-BI)-deficient mice. *J. Clin. Invest.* **108:** 1717–1722.
13. Yesilaltay, A., M. G. Morales, L. Amigo, S. Zanlungo, A. Rigotti, S. L. Karackattu, M. H. Donahee, K. F. Kozarsky, and M. Krieger. 2006. Effects of hepatic expression of the high-density lipoprotein receptor SR-BI on lipoprotein metabolism and female fertility. *Endocrinology.* **147:** 1577–1588.
14. Mardones, P., V. Quinones, L. Amigo, M. Moreno, J. F. Miquel, M. Schwarz, H. E. Miettinen, B. Trigatti, M. Krieger, S. VanPatten, et al. 2001. Hepatic cholesterol and bile acid metabolism and intestinal cholesterol absorption in scavenger receptor class B type I-deficient mice. *J. Lipid Res.* **42:** 170–180.
15. Duggavathi, R., D. H. Volle, C. Mataki, M. C. Antal, N. Messaddeq, J. Auwerx, B. D. Murphy, and K. Schoonjans. 2008. Liver receptor homolog 1 is essential for ovulation. *Genes Dev.* **22:** 1871–1876.
16. Rivera, Z., P. J. Christian, S. L. Marion, H. L. Brooks, and P. B. Hoyer. 2009. Steroidogenic capacity of residual ovarian tissue in 4-vinylcyclohexene diepoxide-treated mice. *Biol. Reprod.* **80:** 328–336.
17. Boyer, A., L. Hermo, M. Paquet, B. Robaire, and D. Boerboom. 2008. Seminiferous tubule degeneration and infertility in mice with sustained activation of WNT/CTNNB1 signaling in Sertoli cells. *Biol. Reprod.* **79:** 475–485.
18. Ramakers, C., J. M. Ruijter, R. H. Deprez, and A. F. Moorman. 2003. Assumption-free analysis of quantitative real-time polymerase chain reaction (PCR) data. *Neurosci. Lett.* **339:** 62–66.
19. Pfaffl, M. W. 2001. A new mathematical model for relative quantification in real-time RT-PCR. *Nucleic Acids Res.* **29:** e45.
20. Littell, R. C., P. R. Henry, and C. B. Ammerman. 1998. Statistical analysis of repeated measures data using SAS procedures. *J. Anim. Sci.* **76:** 1216–1231.
21. Salhab, A. S., B. I. Amro, and M. S. Shomaf. 2003. Further investigation on meloxicam contraceptivity in female rabbits: luteinizing unruptured follicles, a microscopic evidence. *Contraception.* **67:** 485–489.
22. de Duve, C., T. de Barsy, B. Poole, A. Trouet, P. Tulkens, and F. Van Hoof. 1974. Commentary. Lysosomotropic agents. *Biochem. Pharmacol.* **23:** 2495–2531.
23. Stangl, H., G. Cao, K. L. Wyne, and H. H. Hobbs. 1998. Scavenger receptor, class B, type I-dependent stimulation of cholesterol esterification by high density lipoproteins, low density lipoproteins, and nonlipoprotein cholesterol. *J. Biol. Chem.* **273:** 31002–31008.
24. Voshol, P. J., M. Schwarz, A. Rigotti, M. Krieger, A. K. Groen, and F. Kuipers. 2001. Down-regulation of intestinal scavenger receptor class B, type I (SR-BI) expression in rodents under conditions of deficient bile delivery to the intestine. *Biochem. J.* **356:** 317–325.
25. Su, Y. Q., K. Sugiura, K. Wigglesworth, M. J. O'Brien, J. P. Affourtit, S. A. Pangas, M. M. Matzuk, and J. J. Eppig. 2008. Oocyte regulation of metabolic cooperativity between mouse cumulus cells and oocytes: BMP15 and GDF9 control cholesterol biosynthesis in cumulus cells. *Development.* **135:** 111–121.
26. Richards, J. S. 2005. Ovulation: new factors that prepare the oocyte for fertilization. *Mol. Cell. Endocrinol.* **234:** 75–79.
27. Couse, J. F., and K. S. Korach. 2001. Contrasting phenotypes in reproductive tissues of female estrogen receptor null mice. *Ann. N. Y. Acad. Sci.* **948:** 1–8.
28. Sriraman, V., M. Sinha, and J. S. Richards. 2010. Progesterone receptor-induced gene expression in primary mouse granulosa cell cultures. *Biol. Reprod.* **82:** 402–412.
29. Risma, K. A., A. N. Hirshfield, and J. H. Nilson. 1997. Elevated luteinizing hormone in prepubertal transgenic mice causes hyperandrogenemia, precocious puberty, and substantial ovarian pathology. *Endocrinology.* **138:** 3540–3547.
30. Wu, Q., S. Sucheta, S. Azhar, and K. M. Menon. 2003. Lipoprotein enhancement of ovarian theca-interstitial cell steroidogenesis: relative contribution of scavenger receptor class B (type I) and adenosine 5′-triphosphate- binding cassette (type A1) transporter in high-density lipoprotein-cholesterol transport and androgen synthesis. *Endocrinology.* **144:** 2437–2445.
31. Gevry, N., K. Schoonjans, F. Guay, and B. D. Murphy. 2008. Cholesterol supply and SREBPs modulate transcription of the Niemann-Pick C-1 gene in steroidogenic tissues. *J. Lipid Res.* **49:** 1024–1033.
32. Gevry, N., D. Lacroix, J. H. Song, N. Pescador, M. Dobias, and B. D. Murphy. 2002. Porcine Niemann Pick-C1 protein is expressed in steroidogenic tissues and modulated by cAMP. *Endocrinology.* **143:** 708–716.